

# Compact polarimetry in a low frequency spaceborne context

My-Linh Truong-Loï, JPL/Caltech

Anthony Freeman, JPL/Caltech

Pascale Dubois-Fernandez, ONERA

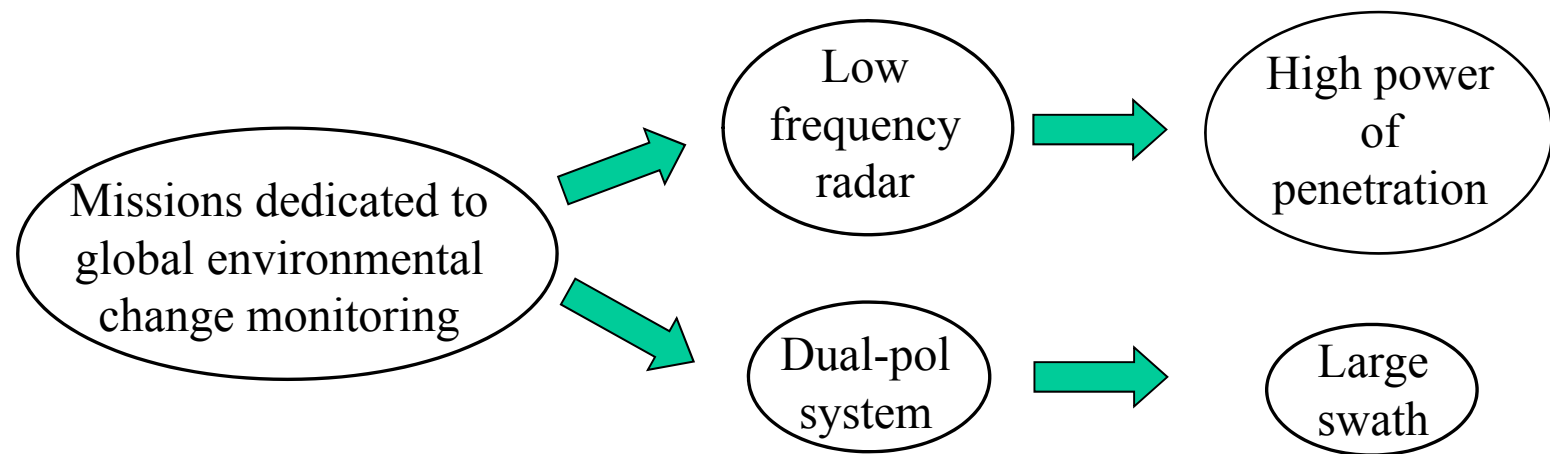
Eric Pottier, IETR, UMR CNRS 6164



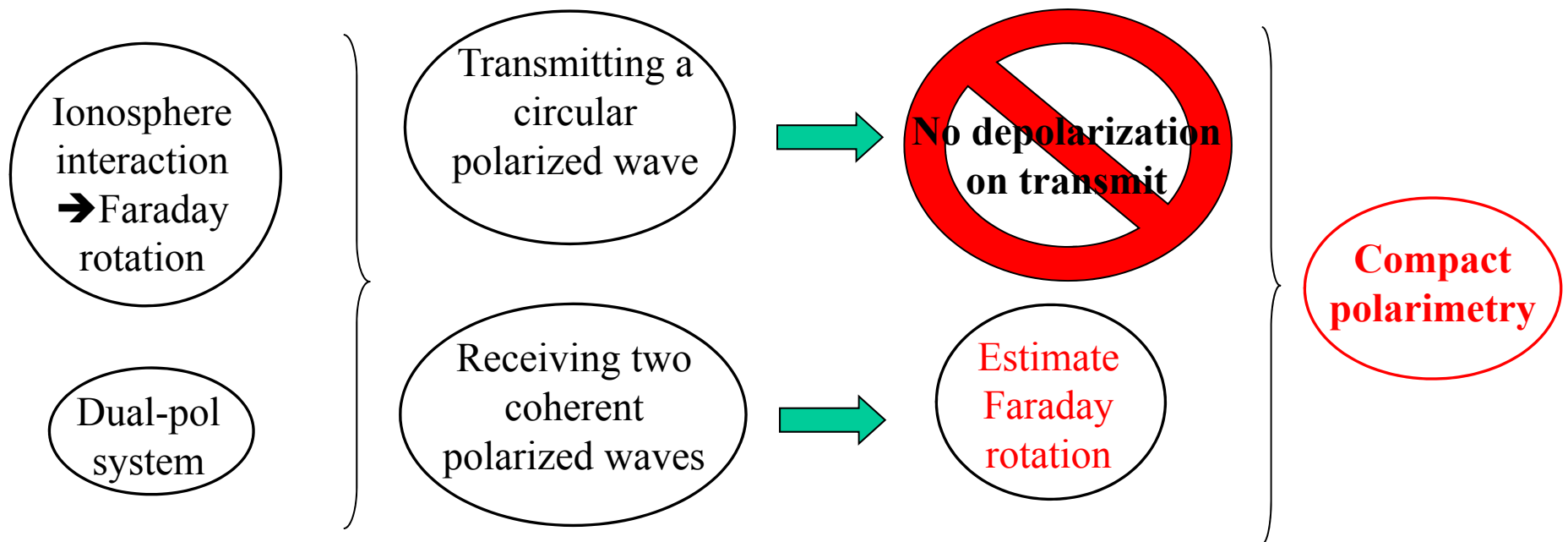
ASAR '11



# Context – restrictions & reasons – 1/2



## Context – restrictions & reasons – 2/2



# Issues

- Compact polarimetry
  - 1 polarization on transmit
  - 2 polarizations on receive
- What is the best polarization on transmit?
- What are the best polarizations on receive?
- How do we analyze the data?
  - Calibration
  - Faraday Rotation
  - Geophysical parameter estimation
    - Compact PolSAR
    - Compact PollnSAR



ASAR '11



# Overview

- Background
- Calibration
- Faraday rotation
- Classification
- Summary



ASAR '11



# Overview

- Background
- Calibration
- Faraday rotation
- Classification
- Summary



ASAR '11



## Background - Example with ALOS system

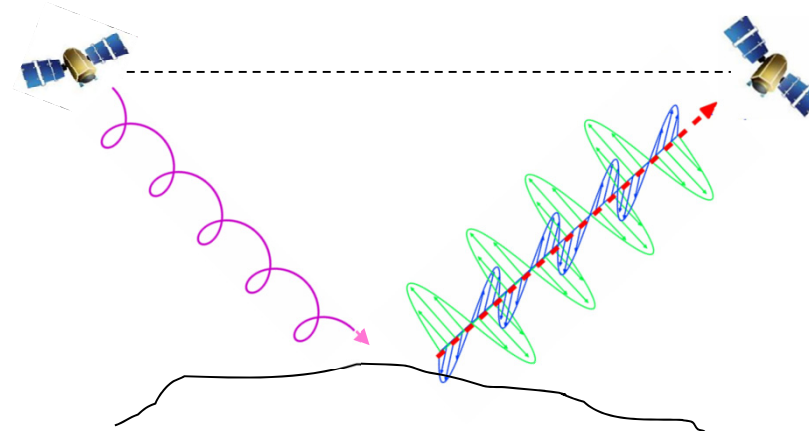
Mode	Swath	Resolution	Incidence angle
HH	70km	10m	8° ~ 60°
HH/HV or VV/VH (dual-pol)	70km	20m	8° ~ 60°
Full polar (quad-pol)	30km	30m	8° ~ 30°

- Single polarisation → large swath and larger incidence angle range
- Full polarisation → added characterisation
- Compact polarisation → full investigation of the dual-pol alternative

φ  
p  
r  
e  
s  
e  
r  
v  
i  
n  
g

# Background - Compact Polarimetry 1/2

- $\pi/4$  mode: one transmission at  $45^\circ$  and two coherent polarizations in reception (linear H & V, circular right & left,...)



# Background - Compact Polarimetry 2/2

- $\pi/4$ -mode potentials: reconstruction of the PolSAR information (1)
  - Iterative algorithm based on:
    - Reflection symmetry
    - Coherence between co-polarized channels
- $\pi/2$ -mode potentials: avoid Faraday rotation in transmission (2)
  - Transmit a circular polarized wave
  - Show results about the reconstruction of the PolSAR information from  $\pi/2$  mode
- Hybrid polarity potentials: decomposition of natural targets (3)
  - $m-\delta$  method based on Stokes parameters

- (1) J-C. Souyris, P. Imbo, R. FjØrtoft, S. Mingot and J-S. Lee, *Compact Polarimetry Based on Symmetry Properties of Geophysical Media: The  $\pi/4$  Mode*, IEEE Transactions on Geoscience and Remote Sensing, vol. 43, no. 3, March 2005.
- (2) P. C. Dubois-Fernandez, J-C. Souyris, S. Angelliaume et F. Garestier, *The Compact Polarimetry Alternative for Spaceborne SAR at Low Frequency*, IEEE Transactions on Geoscience and Remote Sensing, vol. 46, no. 10, October 2008.
- (3) R. K. Raney, *Hybrid-Polarity SAR Architecture*, IEEE Transactions on Geoscience and Remote Sensing, vol. 45, no. 11, November 2007.



ASAR '11



# Overview

- Background
- Calibration
- Faraday rotation
- Classification
- Summary



ASAR '11



# Calibration – Full-pol system

- Full-pol system calibration : 7 unknowns  $\delta_1, \delta_2, \delta_3, \delta_4, \Omega, f_1, f_2$

$$M = A(r, \theta) e^{j\varphi} D_R R_\Omega S R_\Omega D_T + N$$

$$M = A(r, \theta) e^{j\varphi} \begin{pmatrix} 1 & \delta_2 \\ \delta_1 & f_1 \end{pmatrix} \begin{pmatrix} \cos \Omega & \sin \Omega \\ -\sin \Omega & \cos \Omega \end{pmatrix} \begin{pmatrix} S_{HH} & S_{VH} \\ S_{HV} & S_{VV} \end{pmatrix} \begin{pmatrix} \cos \Omega & \sin \Omega \\ -\sin \Omega & \cos \Omega \end{pmatrix} \begin{pmatrix} 1 & \delta_3 \\ \delta_4 & f_2 \end{pmatrix} + N$$

- The S matrix can be recovered:

$$S = R_\Omega^{-1} D_R^{-1} M D_T^{-1} R_\Omega^{-1}$$

- Distortions can be retrieved with measures over known targets:
  - Trihedral, dihedral, transponder, natural targets, etc.

A. Freeman et T. Ainsworth, *Calibration of longer wavelength polarimetric SARs*, Proceedings of EUSAR 2008, Friedrishafen, Allemagne, June 2008.

S. Quegan, *A Unified Algorithm for Phase and Cross-Talk Calibration of Polarimetric Data – Theory and Observations*, IEEE Transactions on Geoscience and Remote Sensing, vol. 32, no. 1, pp. 89-99, January 1994.

J. J. van Zyl, *Calibration of Polarimetric Radar Images Using Only Image Parameters and Trihedral Corner Reflector Responses*, IEEE Transactions on Geoscience and Remote Sensing, vol. 28, no. 3, pp. 337-348, May 1990.



ASAR '11



# Calibration – Compact-pol system

- Compact polarimetric system:

$$M = \frac{1}{\sqrt{2}} A(r, \theta) e^{j\varphi} D_R R_\Omega S R_\Omega D_T \begin{pmatrix} 1 \\ -j \end{pmatrix} + N$$

$$\tilde{R}_\Omega^{-1} \tilde{D}_R^{-1} M = \frac{1}{\sqrt{2}} S R_\Omega D_T \begin{pmatrix} 1 \\ -j \end{pmatrix}$$

# Calibration – Compact-pol system

$$M \cong Ae^{j\varphi}e^{-j\Omega} \frac{1}{\sqrt{2}} \begin{pmatrix} S_{HH}(\cos \Omega - \delta_1 \sin \Omega) - jS_{VV}(\sin \Omega + \delta_1 \cos \Omega) \\ S_{HH}(\delta_2 \cos \Omega - f_1 \sin \Omega) - jS_{VV}(\delta_2 \sin \Omega + f_1 \cos \Omega) \end{pmatrix} + Ae^{j\varphi} \begin{pmatrix} S_{HV}(-j + \delta_1) \\ S_{HV}(-j\delta_2 + f_1) \end{pmatrix}$$

- Compact polarisation
  - 3 reference targets are necessary
    - Dihedral @ 0°
    - Dihedral @ 45°
    - Trihedral
- Full polarisation
  - More unknowns
  - But less targets are required
  - Natural targets can be used
  - Acquisition of both HV and VH



ASAR '11



# Overview

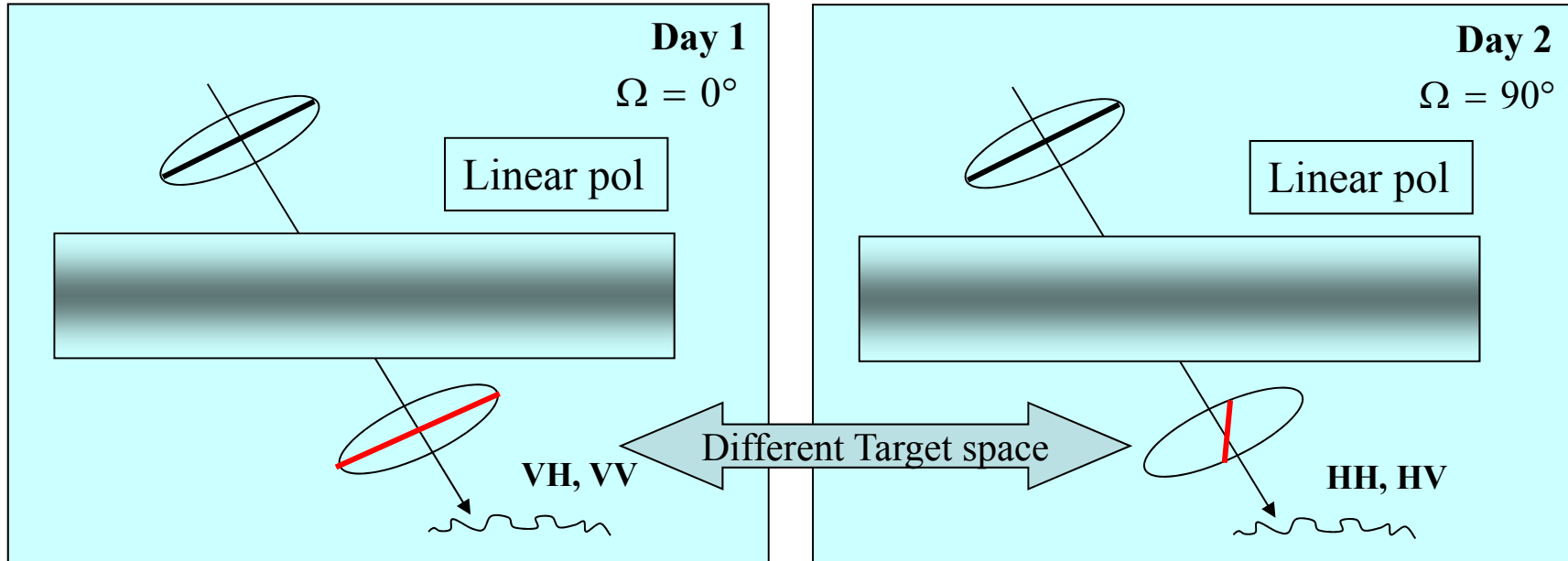
- Background
- Calibration
  - Description and suggested approach
- Faraday rotation
- Classification
- Summary



ASAR '11



# Faraday rotation – Illustration of ionosphere effect



# Faraday rotation estimate using bare soil hypotheses

- Assuming a right circular wave in transmission:

$$\vec{J}_t = \begin{pmatrix} \cos\Omega & \sin\Omega \\ -\sin\Omega & \cos\Omega \end{pmatrix} \overrightarrow{J}_{RC} = \frac{1}{\sqrt{2}} \begin{pmatrix} \cos\Omega & \sin\Omega \\ -\sin\Omega & \cos\Omega \end{pmatrix} \begin{pmatrix} 1 \\ -j \end{pmatrix} = \frac{1}{\sqrt{2}} e^{-j\Omega} \overrightarrow{J}_{RC}$$

- Then the reception is:

$$\vec{k} = \begin{pmatrix} k_1 \\ k_2 \end{pmatrix} = \frac{1}{\sqrt{2}} \begin{pmatrix} \cos\Omega & \sin\Omega \\ -\sin\Omega & \cos\Omega \end{pmatrix} \begin{pmatrix} S_{HH} & S_{HV} \\ S_{VH} & S_{VV} \end{pmatrix} \begin{pmatrix} \cos\Omega & \sin\Omega \\ -\sin\Omega & \cos\Omega \end{pmatrix} \begin{pmatrix} 1 \\ -j \end{pmatrix} = \frac{1}{\sqrt{2}} M \begin{pmatrix} 1 \\ -j \end{pmatrix}$$

$$\vec{k} = \begin{pmatrix} k_1 \\ k_2 \end{pmatrix} = \frac{1}{\sqrt{2}} e^{-j\Omega} \begin{pmatrix} S_{HH} \cos\Omega - j S_{VV} \sin\Omega - j e^{j\Omega} S_{HV} \\ -S_{HH} \sin\Omega - j S_{VV} \cos\Omega + e^{j\Omega} S_{VH} \end{pmatrix}$$

# Overview

- Background
- Calibration
  - Description and suggested approach
- Faraday rotation
  - Some basic properties
  - ...
- Classification
- Summary

# Overview

- Background
- Calibration
  - Description and suggested approach
- Faraday rotation
  - Some basic properties
  - Bare surface hypotheses
- Classification
- Summary



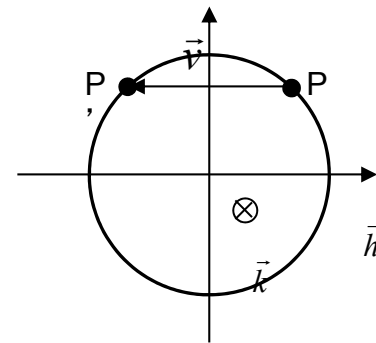
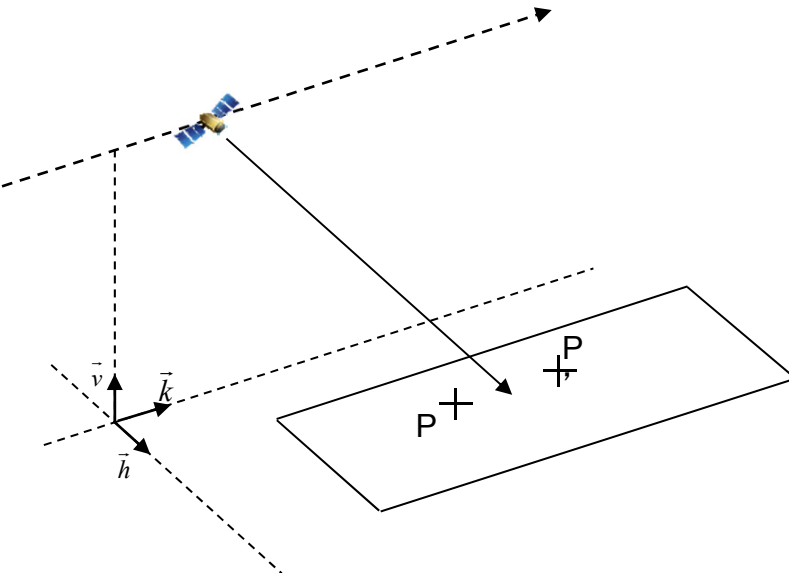
ASAR '11



# Bare surfaces hypotheses

- Using bare soil hypotheses:

- Reflection symmetry:  $\langle S_{HH} S_{HV}^* \rangle \approx \langle S_{VV} S_{HV}^* \rangle \approx 0$
- Bare soil assumption\*:  $\text{Arg} \langle S_{HH} S_{VV}^* \rangle \approx 0$  for incidence angles  $< 40^\circ$



*Reflection symmetry*

\*A. Guissard, "Phase calibration of polarimetric radars from slightly rough surfaces," IEEE Trans. Geosci. Remote Sens., vol. 32, no. 3, pp. 712–714, May 1994.

# Selecting bare surfaces

- Ionosphere interaction

$$M = \begin{pmatrix} M_{RH} \\ M_{RV} \end{pmatrix} = \frac{1}{\sqrt{2}} R_\Omega S R_\Omega \begin{pmatrix} 1 \\ -j \end{pmatrix} = \frac{1}{\sqrt{2}} \begin{pmatrix} \cos \Omega & \sin \Omega \\ -\sin \Omega & \cos \Omega \end{pmatrix} \begin{pmatrix} S_{HH} & S_{HV} \\ S_{HV} & S_{VV} \end{pmatrix} \begin{pmatrix} \cos \Omega & \sin \Omega \\ -\sin \Omega & \cos \Omega \end{pmatrix} \begin{pmatrix} 1 \\ -j \end{pmatrix}$$

$$S = \begin{pmatrix} S_{RH} \\ S_{RV} \end{pmatrix} = \frac{1}{\sqrt{2}} S \begin{pmatrix} 1 \\ -j \end{pmatrix} = \frac{1}{\sqrt{2}} \begin{pmatrix} S_{HH} & S_{HV} \\ S_{HV} & S_{VV} \end{pmatrix} \begin{pmatrix} 1 \\ -j \end{pmatrix}$$

$$\langle M_{RH} M_{RH}^* \rangle \cong \frac{1}{2} \left( |S_{HH}|^2 \cos^2 \Omega + |S_{HV}|^2 + |S_{VV}|^2 \sin^2 \Omega + j \operatorname{Im}(S_{HH} S_{VV}^*) \cos \Omega \sin \Omega \right)$$

$$\langle M_{RV} M_{RV}^* \rangle \cong \frac{1}{2} \left( |S_{HH}|^2 \sin^2 \Omega + |S_{HV}|^2 + |S_{VV}|^2 \cos^2 \Omega - j \operatorname{Im}(S_{HH} S_{VV}^*) \sin \Omega \cos \Omega \right)$$

$$\boxed{\langle S_{RH} S_{RH}^* \rangle + \langle S_{RV} S_{RV}^* \rangle = \langle M_{RH} M_{RH}^* \rangle + \langle M_{RV} M_{RV}^* \rangle \cong \frac{1}{2} \left( |S_{HH}|^2 + 2|S_{HV}|^2 + |S_{VV}|^2 \right)}$$

$$\langle M_{RH} M_{RV}^* \rangle \cong \frac{1}{2} \left( |S_{VV}|^2 - |S_{HH}|^2 \right) \cos \Omega \sin \Omega + j S_{HH} S_{VV}^* \cos^2 \Omega - j |S_{HV}|^2 + j S_{VV} S_{HH}^* \sin^2 \Omega$$

$$\operatorname{Re} \langle M_{RH} M_{RV}^* \rangle \cong \frac{1}{2} \left( \left( |S_{VV}|^2 - |S_{HH}|^2 \right) \cos \Omega \sin \Omega - \operatorname{Im}(S_{HH} S_{VV}^*) (\cos^2 \Omega - \sin^2 \Omega) \right)$$

$$\boxed{\operatorname{Im} \langle S_{RH} S_{RV}^* \rangle = \operatorname{Im} \langle M_{RH} M_{RV}^* \rangle \cong \frac{1}{2} \left( \operatorname{Re}(S_{HH} S_{VV}^*) - |S_{HV}|^2 \right)}$$

# Selecting bare surfaces - The conformity coefficient

Definition

$$\mu = \frac{2 \operatorname{Im} \langle M_{RH} M_{RV}^* \rangle}{\langle M_{RH} M_{RH}^* \rangle + \langle M_{RV} M_{RV}^* \rangle}$$



ASAR '11



# Selecting bare surfaces - The conformity coefficient

$$\mu = \frac{2 \operatorname{Im} \langle M_{RH} M_{RV}^* \rangle}{\langle M_{RH} M_{RH}^* \rangle + \langle M_{RV} M_{RV}^* \rangle} \approx 2 \frac{\operatorname{Re}(S_{HH} S_{VV}^*) - |S_{HV}|^2}{(|S_{HH}|^2 + 2|S_{HV}|^2 + |S_{VV}|^2)}$$



ASAR '11



# Selecting bare surfaces - Four bare surfaces criteria

- Reference criterion:
- Reconstructed ratio HV/VV using JC Souyris\* hypotheses:



HV overestimated

- Coherence between  $M_{RH}$  and  $M_{RV}$ :

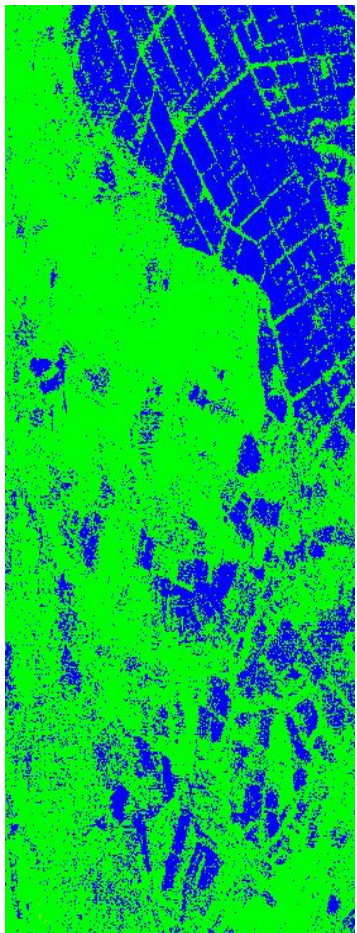
$$\gamma_{M_{RH} M_{RV}^*} = \frac{\langle M_{RH} M_{RV}^* \rangle}{\sqrt{\langle M_{RH} M_{RH}^* \rangle \langle M_{RV} M_{RV}^* \rangle}}$$

- Conformity coefficient:

$$\mu = \frac{2 \operatorname{Im} \langle M_{RH} M_{RV}^* \rangle}{\langle M_{RH} M_{RH}^* \rangle + \langle M_{RV} M_{RV}^* \rangle}$$

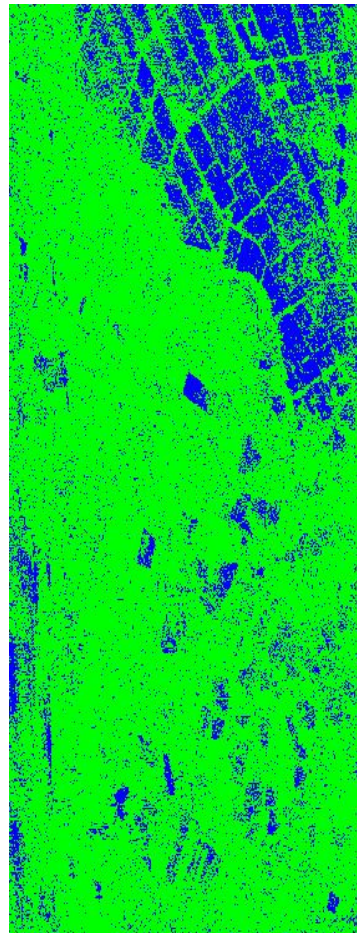
\*J-C. Souyris, P. Imbo, R. FjØrtoft, S. Mingot and J-S. Lee, *Compact Polarimetry Based on Symmetry Properties of Geophysical Media : The  $\pi/4$  Mode*, IEEE Transactions on Geoscience and Remote Sensing, vol. 43, no. 3, March 2005.

# Selecting bare surfaces - The indicators



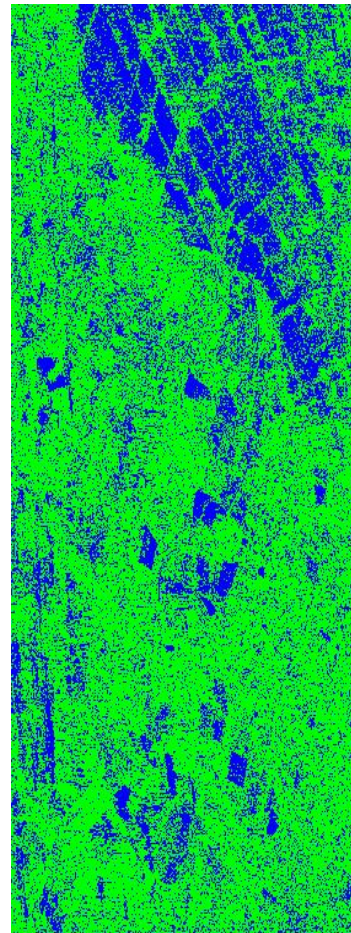
-11dB

$$\frac{\sigma_{HV}^0}{\sigma_{VV}^0}$$



-11dB

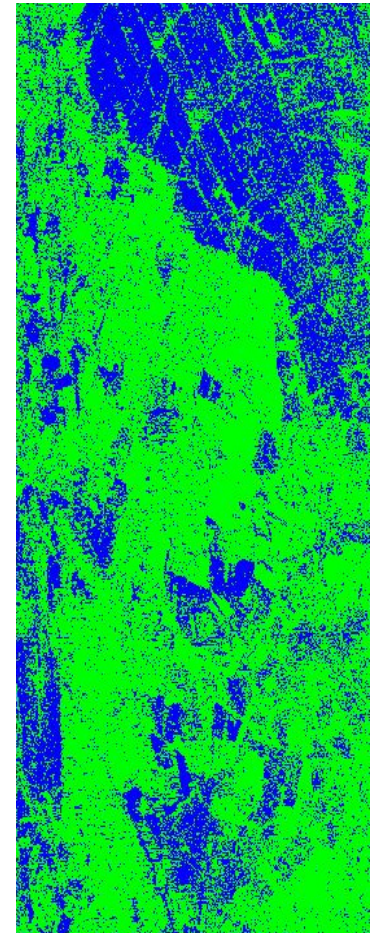
$$\frac{\sigma_{HV}^0}{\sigma_{VV}^0}$$



0 0.61 1

$$\gamma_{M_{RH} M_{RV}^*}$$

ASAR '11



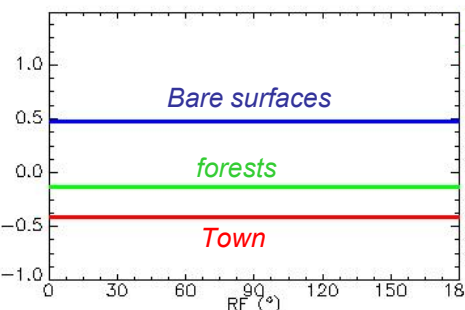
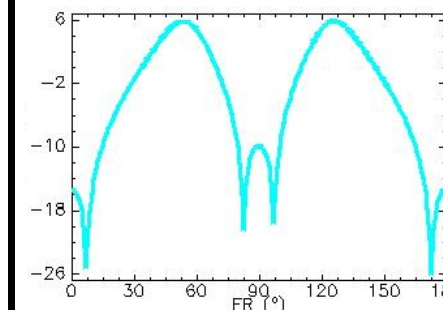
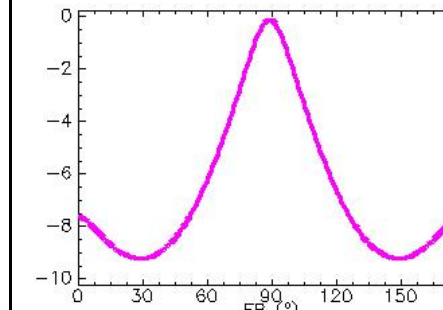
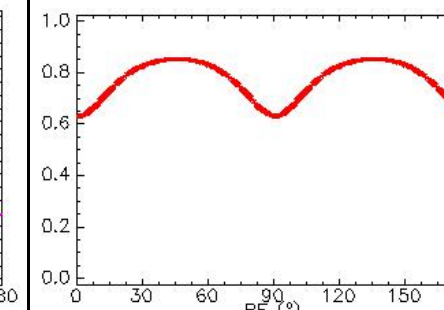
-1 0.3 1

$$\mu$$

JPL

ONERA  
THE FRENCH AEROSPACE LAB

# Selecting bare surfaces - Comparison of four indicators

	$\frac{\sigma_{HV}^0}{\sigma_{VV}^0}$	$\frac{\sigma_{HV}^0}{\sigma_{VV}^0}$	$\gamma_{M_{RH}M_{RV}^*}$	
$\mu$	$\begin{bmatrix} 20.12\% & 12.70\% \\ 12.68\% & 54.50\% \end{bmatrix}$	$\begin{bmatrix} 14.16\% & 5.54\% \\ 32.86\% & 47.44\% \end{bmatrix}$	$\begin{bmatrix} 23.62\% & 8.54\% \\ 15.67\% & 52.17\% \end{bmatrix}$	
	 <p>Plot showing RF (°) from 0 to 180 on the x-axis and value on the y-axis. Three horizontal lines represent different surface types: 'Bare surfaces' (blue, ~0.5), 'forests' (green, ~0), and 'Town' (red, ~-0.5).</p>	 <p>Plot showing RF (°) from 0 to 180 on the x-axis and value on the y-axis. A cyan curve shows two peaks at approximately 60° and 120°, with deep troughs around 90°.</p>	 <p>Plot showing RF (°) from 0 to 180 on the x-axis and value on the y-axis. A magenta curve shows a single sharp peak at approximately 90°.</p>	 <p>Plot showing RF (°) from 0 to 180 on the x-axis and value on the y-axis. A red curve shows a smooth, periodic oscillation between approximately 0.6 and 0.8.</p>

# Overview

- Background
- Calibration
  - Description and suggested approach
- Faraday rotation
  - Some basic properties
  - Bare surfaces requirement → conformity coefficient
  - ...
- Classification
- Summary



ASAR '11



# Overview

- Background
- Calibration
  - Description and suggested approach
- Faraday rotation
  - Some basic properties
  - Bare surfaces requirement → conformity coefficient
  - Faraday rotation estimate
- Classification
- Summary

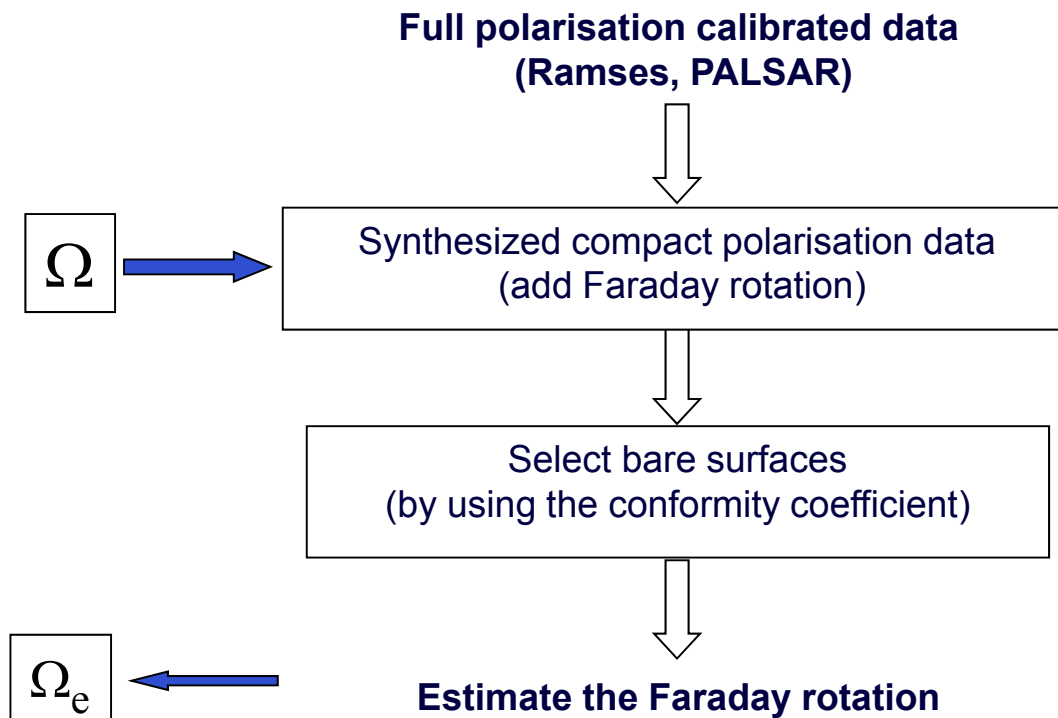


ASAR '11



# Process

- Flow diagram of the process



# Faraday rotation estimate

- Using full polarisation data

- Freeman method (2004,FP data)  $\Omega = \pm \frac{1}{2} \tan^{-1} \sqrt{\frac{4 \langle Z_{HV} Z_{HV}^* \rangle}{\langle M_{HH} M_{HH}^* \rangle + \langle M_{VV} M_{VV}^* \rangle + 2 \operatorname{Re} \langle M_{HH} M_{VV}^* \rangle}} \pm \frac{\pi}{4}$   
with  $Z_{hv}=0.5(M_{vh}-M_{hv})$

- Bickel and Bates (FP linear data transformed in circular basis)

$$\Omega = \frac{1}{4} \arg \langle M_{RL} M_{LR}^* \rangle \pm \frac{\pi}{4}$$



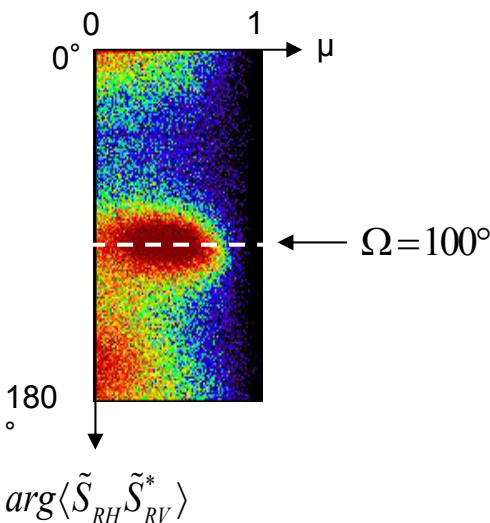
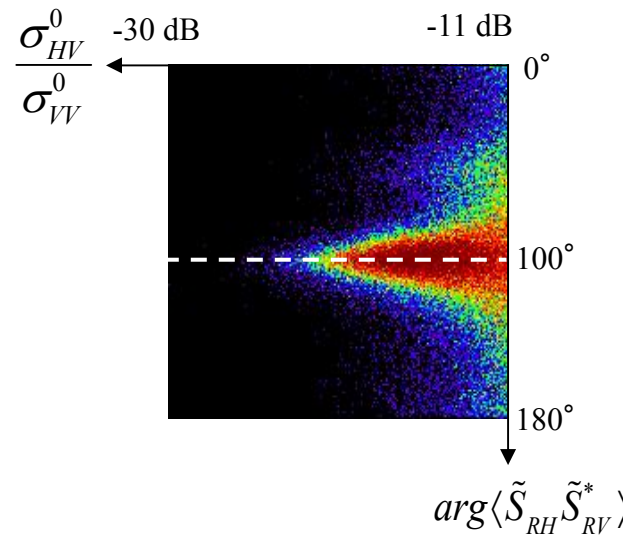
ASAR '11



# Faraday rotation estimate over RAMSES P-band data

$$\Omega=100^\circ$$

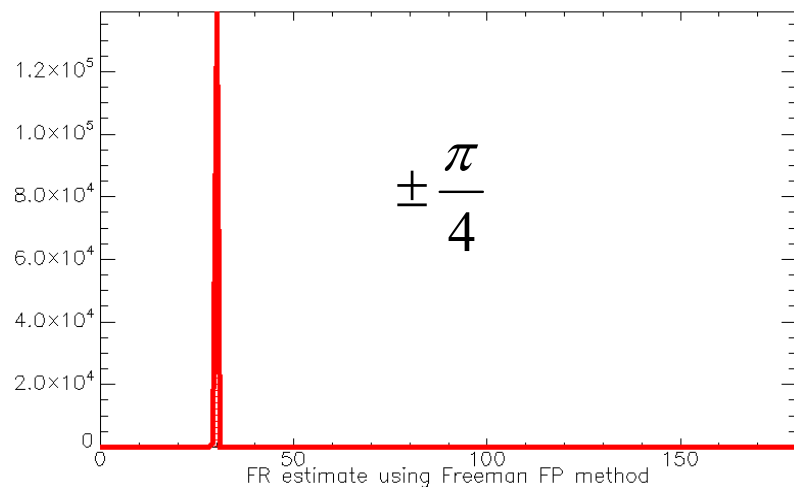
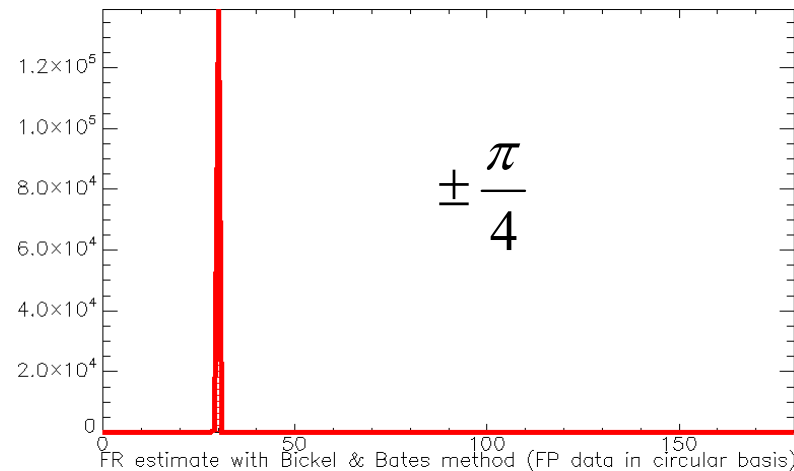
$$\arg\left\langle \tilde{S}_{RH}\tilde{S}_{RV}^* \right\rangle = 90^\circ \pm 180^\circ$$



# Faraday rotation estimate over PALSAR L-band data

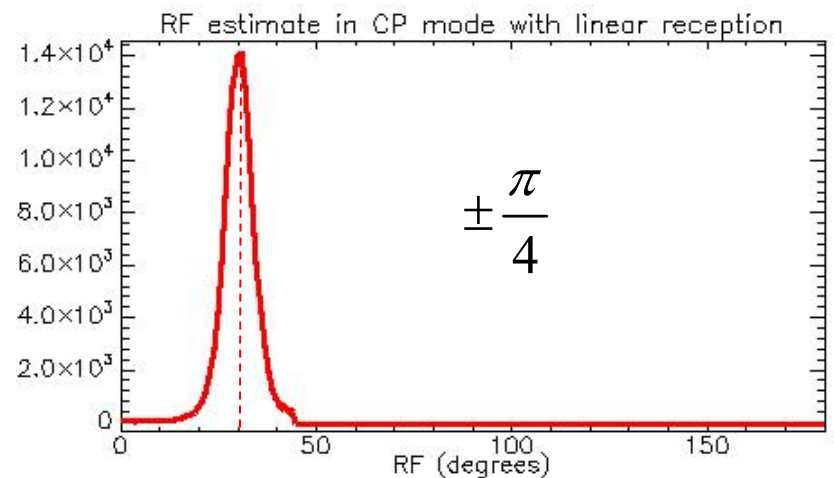
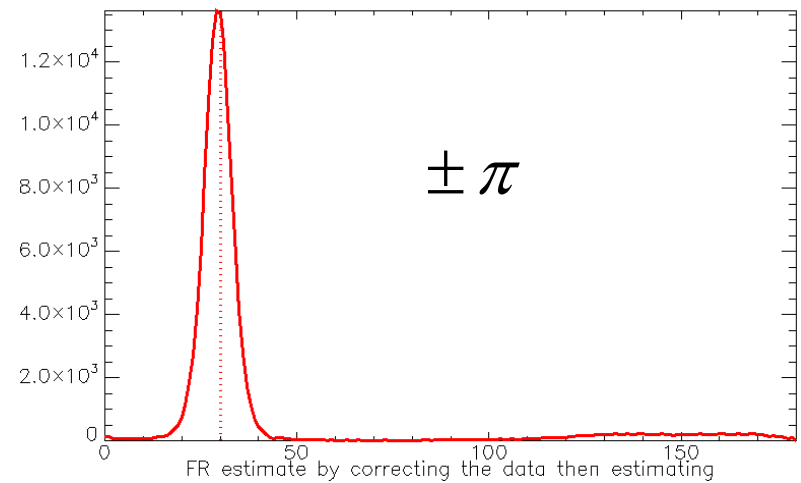
**Full polarimetric data**

$$\Omega=30^\circ$$



**Compact polarimetric data**

Over bare surfaces  $\mu > 0.3$



# Overview

- Background
- Calibration
  - Description and suggested approach
- Faraday rotation
  - Some basic properties
  - Bare surfaces requirement → conformity coefficient
  - Faraday rotation estimate
- Classification
- Summary



ASAR '11



# Overview

- Background
- Calibration
  - Description and suggested approach
- Faraday rotation
  - Some basic properties
  - Bare surfaces requirement → conformity coefficient
  - Faraday rotation estimate
- Classification
- Summary



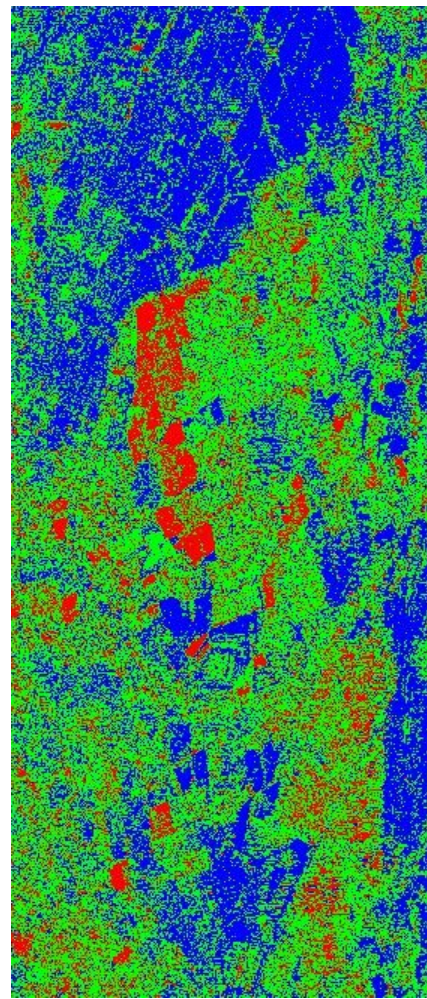
ASAR '11



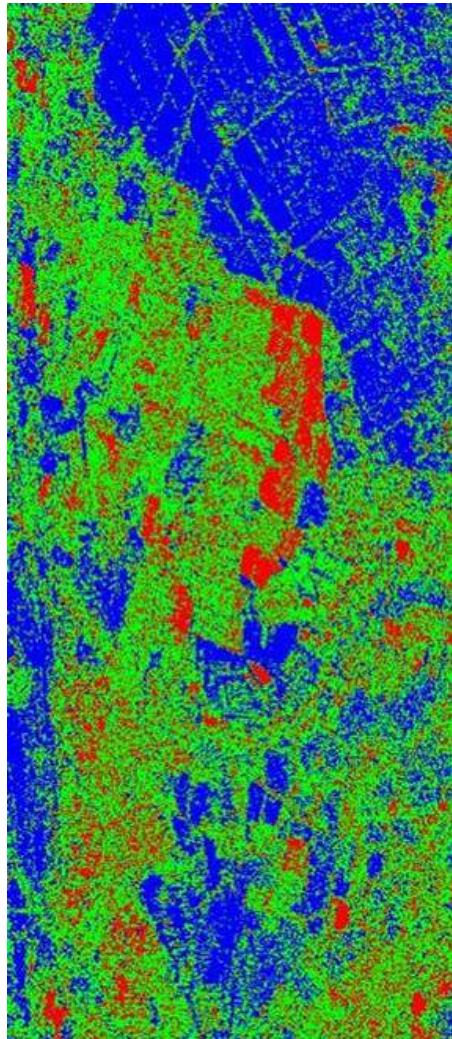
# The conformity coefficient – $\mu$ classifier

$$\mu = \frac{2 \operatorname{Im} \langle M_{RH} M_{RV}^* \rangle}{\langle M_{RH} M_{RH}^* \rangle + \langle M_{RV} M_{RV}^* \rangle} \approx 2 \frac{\operatorname{Re}(S_{HH} S_{VV}^*) - |S_{HV}|^2}{(|S_{HH}|^2 + 2|S_{HV}|^2 + |S_{VV}|^2)}$$

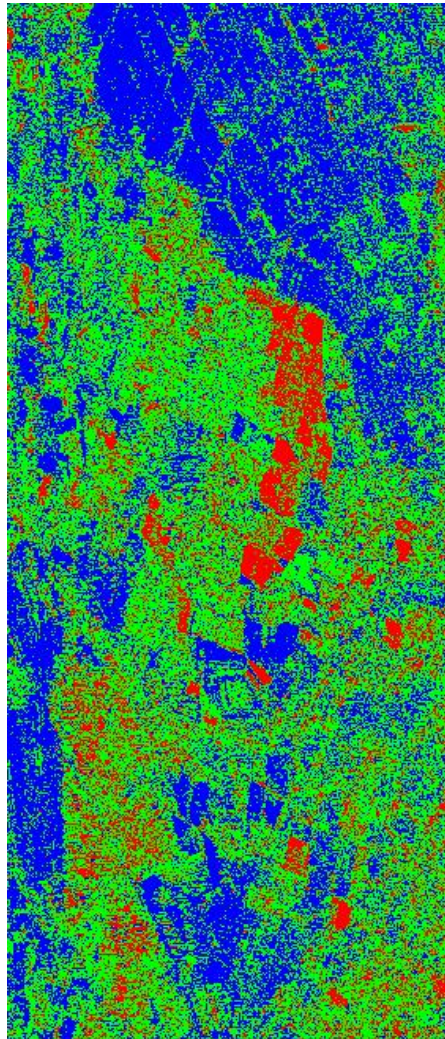
# $\mu$ classifier - RAMSES, P-band, St Germain d' Esteuil



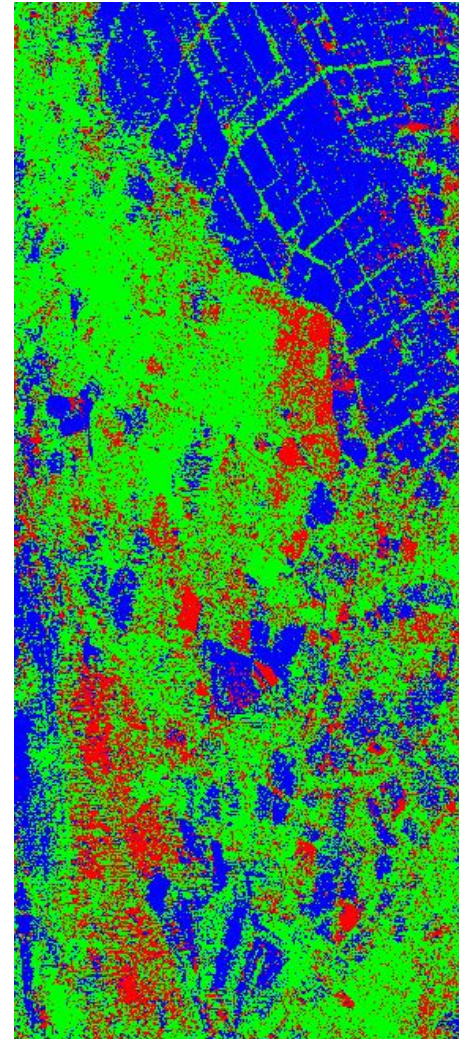
# Qualitative analysis of $\mu$ -classification



*Claude-Pottier classification*



*Conformity coefficient*



*Freeman-Durden classification*

Double-bounce

Volume

Surface

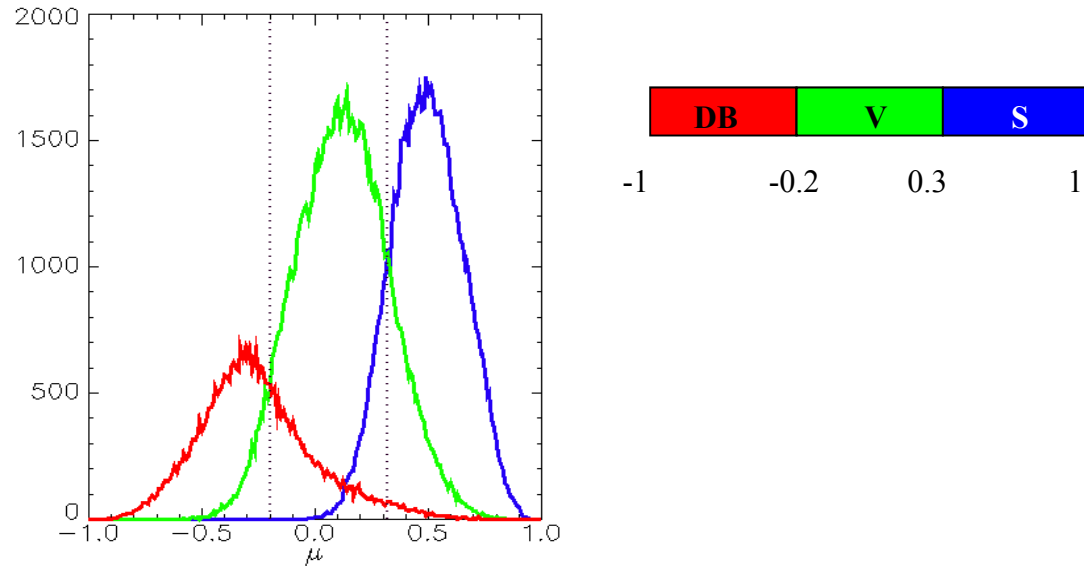
$Pv > 0.6 Pd$  and  $Pv > 0.3 Ps$

$Ps > Pd$



# Quantitative analysis of $\mu$ -classification

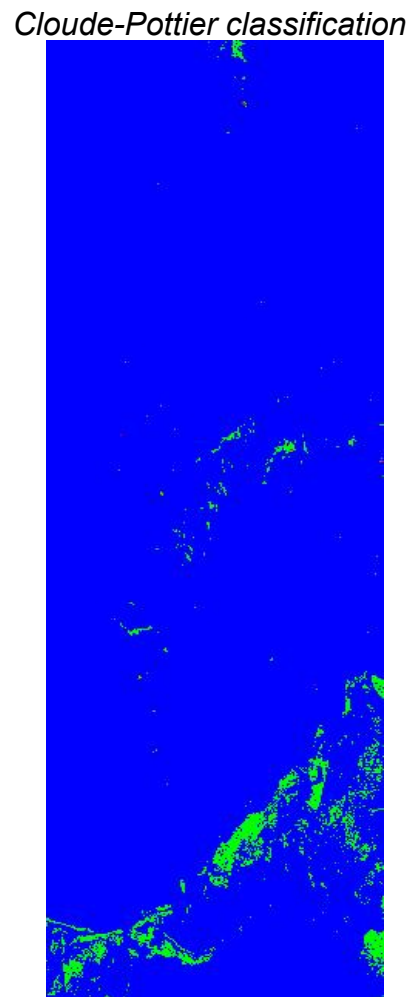
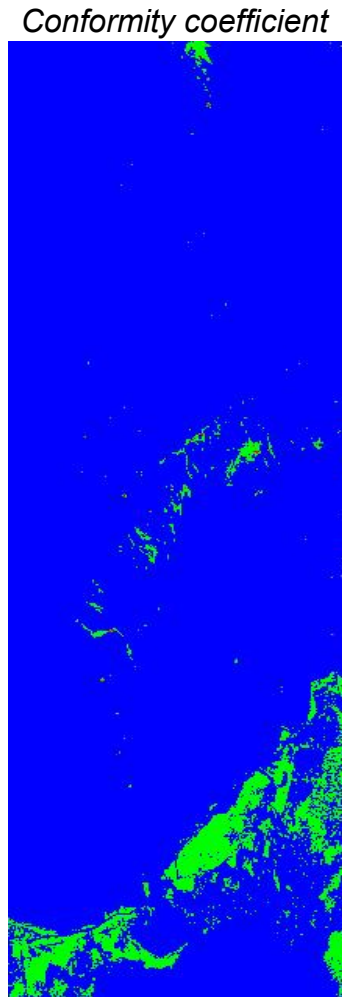
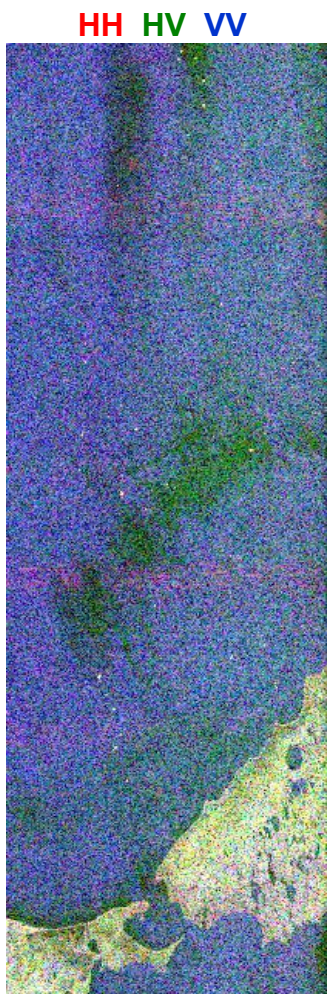
- Conformity coefficient versus Claude-Pottier



- Confusion matrices

$H / \alpha$			$FD$		
	$S$	$V$	$DB$		$S$
$\mu$	$S$	30.31	6.23	0.44	$S$
	$V$	6.66	36.26	2.06	$V$
	$DB$	0.04	6.54	11.46	$DB$

# $\mu$ classifier over PALSAR L-band data



$H / \alpha$

	$S$	$V$	$DB$
$S$	94.23	0.01	0.00
$\mu$	3.12	2.61	0.00
$DB$	0.00	0.02	0.01

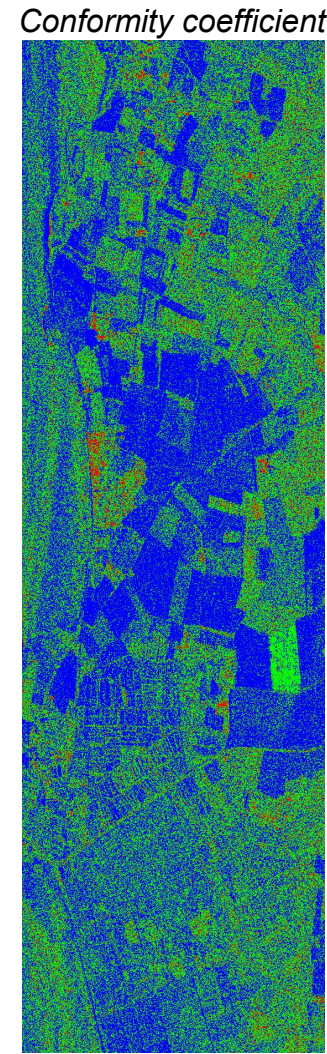
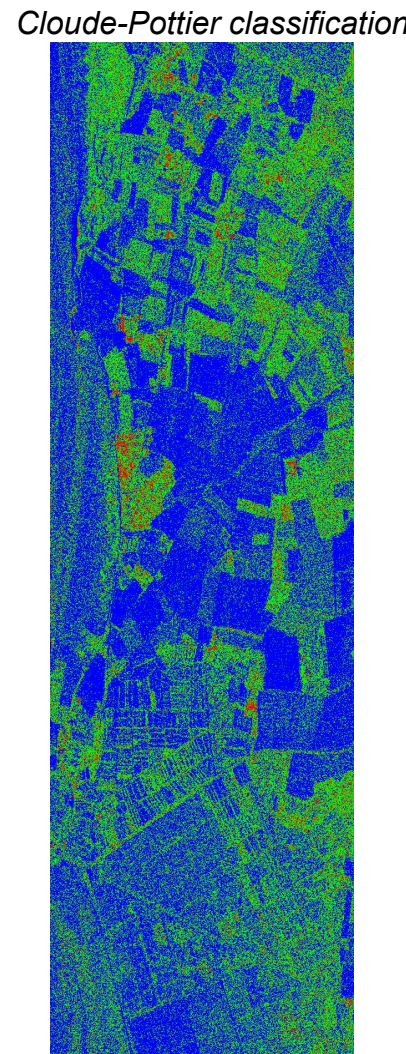
Double-bounce      Volume      Surface

JPL

ASAR '11



# $\mu$ classifier over RAMSES L-band data, Le Moulin du Fâ



$H / \alpha$

	$S$	$V$	$DB$
$S$	43.2	2.62	0.08
$\mu$	12.89	32.2	1.67
$DB$	0.00	2.31	4.96

Double-bounce

Volume

Surface

JPL

ASAR '11

IETR  
INSTITUT D'ÉLECTRONIQUE ET DE TÉLÉCOMMUNICATIONS DE RENNES

ONERA  
THE FRENCH AEROSPACE LAB

# Overview

- Background
- Calibration
  - Description and suggested approach
- Faraday rotation
  - Some basic properties
  - Bare surfaces requirement → conformity coefficient
  - Faraday rotation estimate
- Classification
  - Classification using the conformity coefficient
  - ...
- Summary



ASAR '11



# Overview

- Background
- Calibration
  - Description and suggested approach
- Faraday rotation
  - Some basic properties
  - Bare surfaces requirement → conformity coefficient
  - Faraday rotation estimate
- Classification
  - Classification using the conformity coefficient
  - Classification of different types of vegetation
- Summary

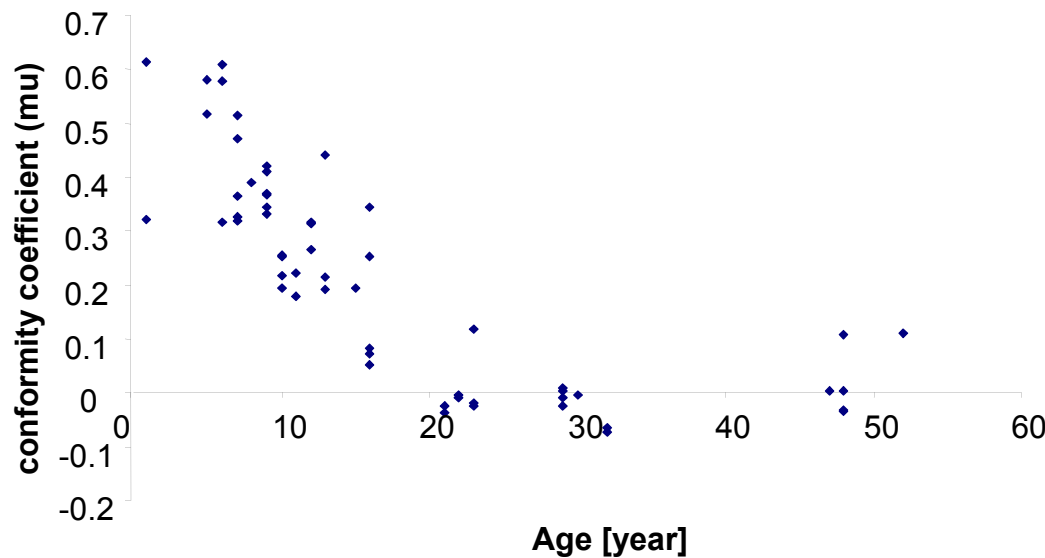


ASAR '11



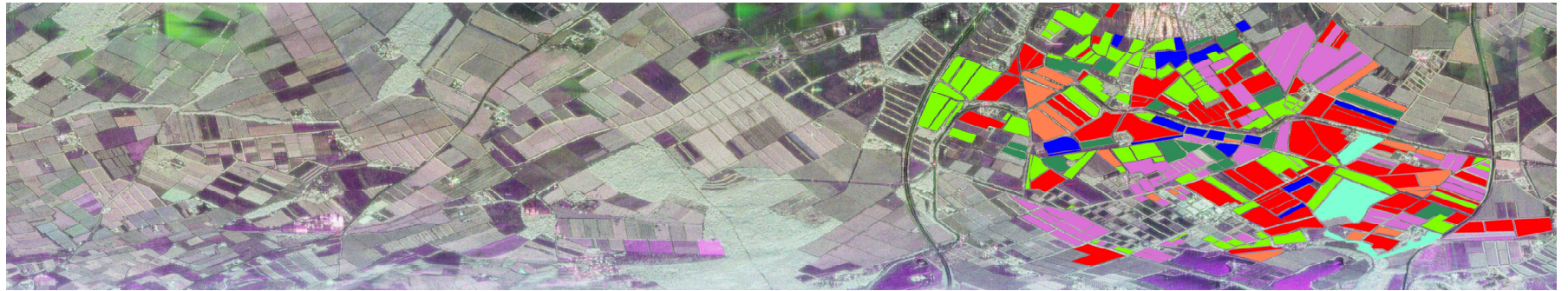
# Behavior of $\mu$ with forest ages

RAMSES data, Nezer, 2001, P-band

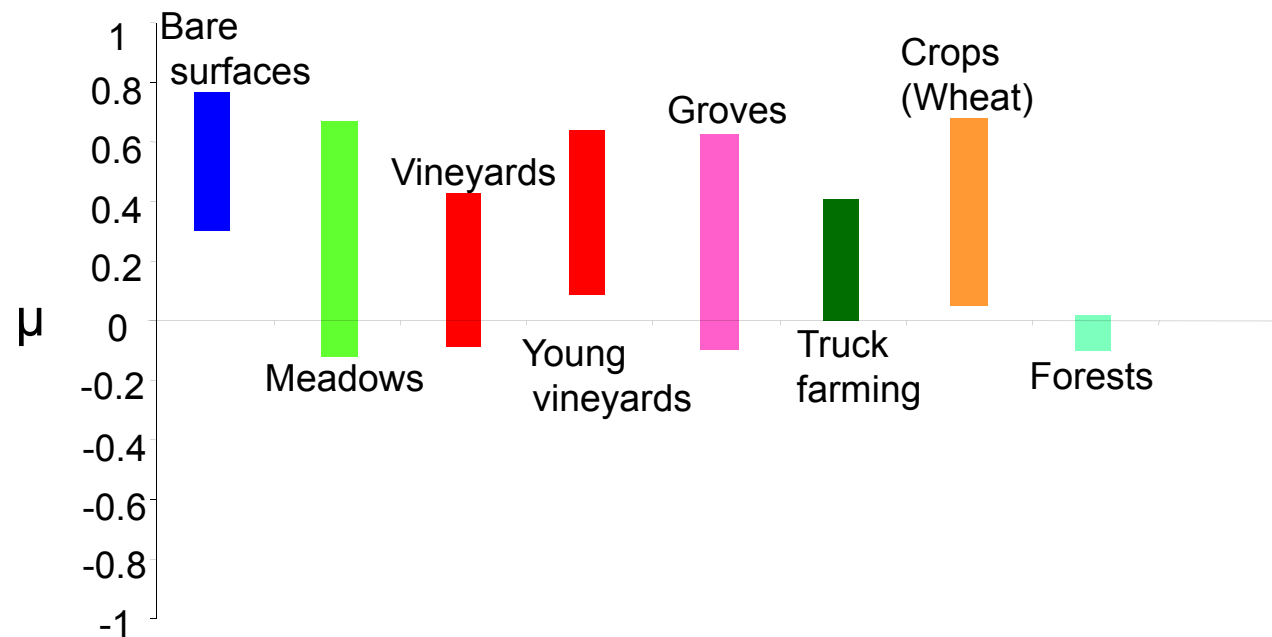


- Young forest plots act as bare surfaces
  - $0.2 < \mu < 1$
- Old forest plots act as volume
  - $\mu \sim 0$

# $\mu$ over different types of vegetation



*SETHI FP data, L-band, Garons*



# Overview

- Background
- Calibration
  - Description and suggested approach
- Faraday rotation
  - Some basic properties
  - Bare surfaces requirement → conformity coefficient
  - Faraday rotation estimate
- Classification
  - Classification using the conformity coefficient
  - Classification of different types of vegetation
- Summary



ASAR '11



# Overview

- Background
- Calibration
  - Description and suggested approach
- Faraday rotation
  - Some basic properties
  - Bare surfaces requirement → conformity coefficient
  - Faraday rotation estimate
- Classification
  - Classification using the conformity coefficient
  - Classification of different types of vegetation
- Summary



ASAR '11



# Summary: systems implications

- Compact-pol allows
  - To acquire larger swath (versus FP)
  - To access wider incidence angle range (versus FP)
  - To avoid Faraday rotation in transmission (versus DP)
- Calibration
  - A solution with 3 external targets
- Estimation of Faraday rotation possible
  - Over bare surfaces selected by the conformity coefficient which
    - Is FR independent
    - Can be used with CP data as well as FP data
    - Allows distinguishing 3 different types of scattering
  - Using 3 methods with circular transmission and two circular OR linear receptions
    - One modulo  $\pi/4$
    - Two modulo  $\pi$